

# Thermal conductivity and interfacial energy of solid Bi in the Bi–Ag eutectic system

Yemliha Altıntaş<sup>1</sup> · Esra Öztürk<sup>2</sup> · Sezen Aksöz<sup>3</sup> · Kâzım Keşlioğlu<sup>4</sup> · Necmettin Maraşlı<sup>5</sup>

Received: 2 January 2015 / Accepted: 19 April 2015 / Published online: 15 May 2015  
© Akadémiai Kiadó, Budapest, Hungary 2015

**Abstract** The equilibrated grain boundary groove shapes for solid Bi (Bi–2.87 at.%Ag) in equilibrium with Bi–Ag eutectic liquid have been observed from quenched sample with a radial heat flow apparatus. The Gibbs–Thomson coefficient, solid–liquid interfacial energy and grain boundary energy of solid Bi have been determined from the observed grain boundary groove shapes. The variation of thermal conductivity with temperature for eutectic solid phase (Bi–4.7 at.%Ag) has been measured. The ratio of thermal conductivity of equilibrated eutectic liquid phase to eutectic solid phase has also been measured with a Bridgman-type growth apparatus at the melting temperature. The Gibbs–Thomson coefficient, solid–liquid interfacial energy and grain boundary energy of solid Bi in equilibrium with Bi–Ag eutectic liquid were determined to be  $(9.2 \pm 0.6) \times 10^{-8}$  K m,  $(52.7 \pm 6.3) \times 10^{-3}$  J m<sup>-2</sup> and  $(102.4 \pm 13.3) \times 10^{-3}$  J m<sup>-2</sup>, respectively, from observed grain boundary groove shapes.

**Keywords** Alloys · Liquid–solid reactions · Grain boundaries · Thermodynamic properties

## Introduction

The solid–liquid interfacial energy,  $\sigma_{sl}$ , is recognized to play a key role in a wide range of metallurgical and materials phenomena from wetting [1] and sintering through to phase transformations and coarsening [2]. Thus, a quantitative knowledge of  $\sigma_{sl}$  values is necessary. However, the determination of  $\sigma_{sl}$  is difficult. Since 1985, a technique for the quantification of solid–liquid interfacial free energy from the grain boundary groove shape has been established and measurements have been reported for several systems [3–10]. The grain boundary groove shape formed at the solid–liquid interface in a thermal gradient can be used to determine the interfacial energy, and the interface near the groove must everywhere satisfy

$$\Delta T_r = \left[ \frac{1}{\Delta S^*} \right] \left[ \left( \sigma_{sl} + \frac{d^2 \sigma_{sl}}{dn_1^2} \right) \kappa_1 + \left( \sigma_{sl} + \frac{d^2 \sigma_{sl}}{dn_2^2} \right) \kappa_2 \right] \quad (1)$$

where  $\Delta T_r$  is the curvature undercooling,  $\Delta S^*$  is the entropy of fusion per unit volume,  $n$  ( $n_x$ ,  $n_y$ ,  $n_z$ ) is the interface normal,  $\kappa_1$  and  $\kappa_2$  are the principal curvatures, and the derivatives are taken along the directions of principal curvature. Equation 1 is valid only if the interfacial free energy per unit area is equal to surface tension per unit length,  $\sigma_{sl} = \gamma$ . When interfacial free energy differs from surface tension, the problem is more complicated and the precise modification of the Gibbs–Thomson equation is not yet established [11]. When the solid–liquid interfacial free energy is isotropic, Eq. 1 becomes

✉ Kâzım Keşlioğlu  
kesli@erciyes.edu.tr

<sup>1</sup> Department of Materials Science and Nanotechnology, Faculty of Engineering, Abdullah Gül University, Kayseri, Turkey

<sup>2</sup> Department of Physics, Faculty of Arts and Science, Kocaeli University, 41380 Kocaeli, Turkey

<sup>3</sup> Department of Physics, Faculty of Arts and Science, Nevşehir Hacı Bektaş Veli University, 50300 Nevşehir, Turkey

<sup>4</sup> Department of Physics, Faculty of Science, Erciyes University, 38039 Kayseri, Turkey

<sup>5</sup> Department of Metallurgical and Materials Engineering, Faculty of Chemical and Metallurgical Engineering, Yıldız Technical University, Davutpaşa, 34210 Istanbul, Turkey

$$\Delta T_r = \frac{\sigma_{sl}}{\Delta S^*} \left( \frac{1}{r_1} + \frac{1}{r_2} \right) \quad (2)$$

where  $r_1$  and  $r_2$  are the principal radii of the curvature. For the case of a planar grain boundary intersecting a planar solid–liquid interface,  $r_2 = \infty$  and Eq. 2 becomes

$$\Gamma = r \Delta T_r = \frac{\sigma_{sl}}{\Delta S^*} \quad (3)$$

where  $\Gamma$  is the Gibbs–Thomson coefficient. This equation is called the Gibbs–Thomson relation [6].

Gündüz and Hunt [6] developed a finite difference model to calculate the Gibbs–Thomson coefficient. This numerical method calculates the temperature along the interface of a measured grain boundary groove shape rather than attempting to predict the equilibrium grain boundary groove shape. If the grain boundary groove shape, the temperature gradient in the solid ( $G_s$ ) and the ratio of thermal conductivity of the equilibrated liquid phase to solid phase ( $R$ ) are known or measured, the value of the Gibbs–Thomson coefficient ( $\Gamma$ ) is then obtained with the Gündüz and Hunt's numerical method.

One of the common techniques for measuring solid–liquid interfacial free energy is the grain boundary groove method. In this technique, the solid–liquid interface is equilibrated with a grain boundary in a temperature gradient as shown in [8], and the mean value of solid–liquid interfacial free energy is obtained from the measurements of equilibrium shape of the groove profile. Over last 25 years, the equilibrated grain boundary groove shapes in variety of materials have been observed and the measurements of the solid–liquid interfacial free energies were made from observed grain boundary groove shapes [3–10].

The phase diagram of bismuth (Bi)–silver (Ag) has been evaluated from [12]. Some thermal properties such as solid–liquid interfacial energy, Gibbs–Thomson coefficient, grain boundary energy and thermal conductivity of solid and liquid phases in the Bi–Ag eutectic system have not been well known. The values of solid–liquid interfacial energy, Gibbs–Thomson coefficient and grain boundary energy could be of use to people doing comparisons between experimentally observed solidification morphology and predictions from theoretical models. Thus the aims of the present work were to observe the equilibrated grain boundary groove shapes for solid Bi in equilibrium with Bi–Ag eutectic liquid and to determine the thermal conductivity of solid and liquid phases, the Gibbs–Thomson coefficient, solid–liquid interfacial energy and grain boundary energy for solid Bi in the Bi–Ag eutectic system.

## Experimental

### Experimental apparatus

In order to observe the equilibrated grain boundary groove shapes in opaque materials, Gündüz and Hunt [6] designed a radial heat flow apparatus. Maraşlı and Hunt [7] improved the experimental apparatus for higher temperature. The details of the apparatus and experimental procedures are given in [6–10]. In the present work, a similar apparatus was used to observe the grain boundary groove shapes in the Bi–Ag eutectic system.

### Sample preparation

From the phase diagram of Bi–Ag alloy, the eutectic liquid composition is Bi–4.7 at.%Ag [12]. The composition of alloy was chosen to be Bi–2.87 at.%Ag to grow the solid Bi phase on the eutectic structure in a short annealing time. Bi–2.87 at.%Ag alloy was prepared in a vacuum furnace by using bismuth and silver. The bismuth and silver that have the purity of 99.99 % were supplied from Alfa Easer. After stirring, the molten alloy was poured into a graphite crucible, held in a specially constructed casting (hot filling) furnace at approximately 50 K above the melting point of alloy. The molten metal was then directionally solidified from bottom to top to ensure that the crucible was completely full. The sample was then placed in the radial heat flow apparatus.

The experiments were carried out in two steps. In the first step, the thermocouples were calibrated by detecting the melting point during very slow heating and cooling. In the second step, the specimen was heated from the centre using a single heating wire (1.7 mm in diameter, Kanthal A-1) and the outside of the specimen was kept at 293 K using a *Poly Science digital 9102* model heating/refrigerating circulating bath. A thin liquid layer (1–2 mm thick) was melted around the central heater, and the specimen was annealed in a very stable temperature gradient for a long time. In this condition, the solid and liquid layers were mixed together. During the annealing period, the liquid droplets move up towards the hot zone of the sample by temperature gradient zone melting and single solid phase can grow. The annealing time for Bi–2.87 at.%Ag was 4 days. During the annealing period, the temperature in the specimen and the vertical temperature variations on the sample were continuously recorded by the stationary thermocouples and a moveable thermocouple, respectively, by using a data logger via computer. The input power was also recorded periodically. The temperature in the sample

was stable to about  $\pm 0.025$  K for hours and  $\pm 0.05$  K for up to 4 days. At the end of the annealing time, the specimen was rapidly quenched by turning off the input power which was sufficient to get a well-defined solid–liquid interface, because the liquid layer around the central heating wire was very thin (typically smaller than 1 mm).

### Measurements of the coordinates of equilibrated grain boundary groove shapes

The quenched sample was cut transversely into lengths typically of 25 mm, and transverse sections were ground flat with 180 grit SiC paper. Grinding and polishing were then carried out by following a standard route. After polishing, the samples were etched with air.

The equilibrated grain boundary groove shapes were then photographed with an *Olympus DP12*-type CCD digital camera placed on top of an *Olympus BX51*-type light optical microscope. A graticule ( $200 \times 0.01 = 2$  mm) was also photographed using the same objective. The photographs of the equilibrated grain boundary groove shapes and the graticule were superimposed on one another using *Adobe PhotoShop 8.0* version software so that accurate measurement of the groove coordinate points on the groove shapes could be made.

The coordinates of equilibrated grain boundary groove shapes were measured by Maraşlı and Hunt's geometrical method [7] so that appropriate corrections to the shape of the grooves could be deduced and the details of the geometrical method are given in [7].

### Measurements of the thermal conductivity of solid phase at its melting temperature

The thermal conductivity ratio of equilibrated eutectic liquid phase (Bi–4.7 at.%Ag) to solid Bi phase,  $R = K_{L(\text{eutectic liquid})}/K_{S(\text{Bi})}$  must be known or measured to evaluate the Gibbs–Thomson coefficient with the Gündüz and Hunt's numerical method. The radial heat flow method is an ideal technique for measuring the thermal conductivity of the solid phase.

The thermal conductivity of eutectic solid phase (Bi–4.7 at.%Ag) was measured in the radial heat flow apparatus. As mentioned above, a specimen which is approximately 100 mm in length and 30 mm in diameter was produced by using the vacuum and hot filling furnaces and then placed in the radial heat flow apparatus.

The thermal conductivity of eutectic solid phase (Bi–4.7 at.%Ag) versus temperature is shown in Fig. 1. A comparison of thermal conductivity of eutectic solid phase with the thermal conductivity of Bi [13] is also shown in Fig. 1. The value of  $K_s$  for eutectic solid phase (Bi–4.7 at.%Ag) at the melting temperature was obtained to be

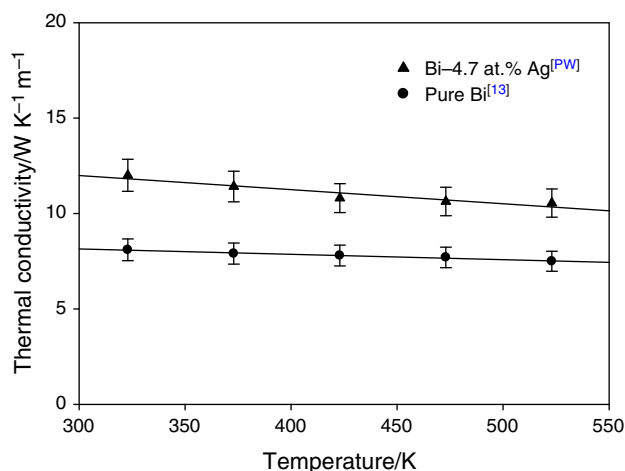


**Fig. 1** Thermal conductivity of eutectic solid phase (Bi–4.7 at.%Ag) versus temperature

$10.44 \text{ W K}^{-1} \text{ m}^{-1}$  by extrapolating the line to the eutectic temperature as shown in Fig. 1.

### The ratio of thermal conductivity of equilibrated liquid phase to solid phase

It is not possible to measure the thermal conductivity of the liquid phase with the radial heat flow apparatus since a thick liquid layer (10 mm) is required. A layer of this size would certainly have led to convection. If the thermal conductivity ratio of the liquid phase to the solid phase is known and the thermal conductivity of the solid phase is measured at the melting temperature, the thermal conductivity of the liquid phase can then be evaluated. The thermal conductivity ratio can be obtained during directional growth with a Bridgman-type growth apparatus [14]. The thermal conductivity ratio,  $R$ , is given by

$$R = \frac{K_l}{K_s} = \frac{G_s}{G_l} \quad (4)$$

A directional growth apparatus, firstly constructed by McCartney [15], was used to find out the thermal conductivity ratio. A thin-walled graphite crucible, 6.3 mm OD  $\times$  4 mm ID  $\times$  180 mm lengths, was used to minimize convection in the liquid phase.

Molten eutectic alloy (Bi–4.7 at.%Ag) was poured into the thin-walled graphite tube. The specimen was then placed in the directional growth apparatus. The specimen was heated to 100 K over the melting temperature of alloy. The specimen was then left to reach thermal equilibrium for at least 2 h. The temperature in the specimen was measured with an insulated K-type thermocouple. In the present work, 1.2 mm OD  $\times$  0.8 mm ID alumina tube was used to insulate the thermocouple from the melt and the thermocouple was placed perpendicular to the heat flow

(growth) direction. When the specimen temperature stabilized, the directional growth was begun by turning the motor on. The cooling rate was recorded with a data logger via computer. When the solid–liquid interface passed the thermocouple, a change in the slope of the cooling rate for liquid and solid phases was observed. When the thermocouple reading was approximately 50 K below the melting temperature, the growth was stopped by turning the motor off. The detail of the experimental procedure was given in [6–10, 16–18].

The thermal conductivity ratio of the eutectic liquid (Bi–4.7 at.%Ag) to the eutectic solid (Bi–4.7 at.%Ag),  $R = K_{l(\text{eutectic})}/K_{s(\text{eutectic})}$ , was measured to be 0.88 with a Bridgman-type growth apparatus and the temperature versus time curve shown in Fig. 2. The thermal conductivity of the eutectic solid at the eutectic temperature was also measured to be  $10.44 \text{ W K}^{-1} \text{ m}^{-1}$ . The thermal conductivity of the eutectic liquid was then determined to be  $9.19 \text{ W K}^{-1} \text{ m}^{-1}$ . Thus, the thermal conductivity ratio of the equilibrated eutectic liquid phase to the solid Bi phase,  $R = K_{l(\text{eutectic liquid})}/K_{s(\text{Bi})}$ , is also found to be 1.45 by using the values of  $K_{l(\text{eutectic})}$  and  $K_{s(\text{Bi})}$  [13]. The thermal conductivities of the solid and liquid phases for solid Bi and Bi–Ag eutectic solid and their ratios used in the determination of the Gibbs–Thomson coefficient are also given in Table 1. A comparison of the values of  $K_s$  and  $K_l$  obtained in the present work with the values of  $K_s$  and  $K_l$  for similar alloy systems is also given in Table 1. As can be seen from Table 1, the results obtained in present work are in good agreement with previous works.

### Determination of temperature gradient in the solid phase

The average temperature gradient of the solid phase must be determined for each grain boundary groove shape. This was done by measuring the input power, the length of heating

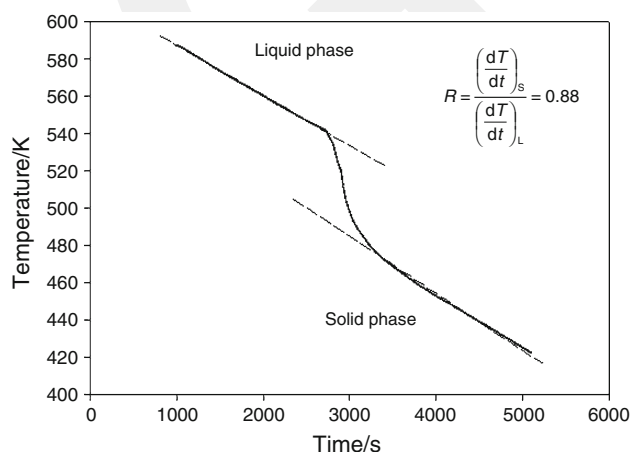


**Fig. 2** Cooling rate of eutectic Bi–4.7 at.%Ag alloy

wire, the position of the solid–liquid interface and the value of  $K_s$  for solid Bi phase at the eutectic melting temperature. By using these measured values, temperature gradient can be determined for each grain boundary groove shape.

The total fractional uncertainty in the measurement of temperature gradient is about 6.5 % [21].

## Results and discussion

### Determination of Gibbs–Thomson coefficient

If the thermal conductivity ratio of equilibrated liquid phase to solid phase, the coordinates of the grain boundary groove shape and the temperature gradient of the solid phase are known, the Gibbs–Thomson coefficient ( $\Gamma$ ) can be obtained using the Gündüz and Hunt’s numerical method described in detail in [6]. The experimental error in the determination of Gibbs–Thomson coefficient is the sum of experimental errors in the measurement of the temperature gradient, thermal conductivity and groove coordinates. Thus the total error in the determination of Gibbs–Thomson coefficient is estimated to be about 7 % [7].

The Gibbs–Thomson coefficients for solid Bi in equilibrium with the eutectic liquid (Bi–4.7 at.%Ag) were determined with Gündüz and Hunt’s numerical model by using ten equilibrated grain boundary groove shapes. Typical grain boundary groove shapes for solid Bi in equilibrium with the eutectic liquid are shown in Fig. 3. The values of  $\Gamma$  for solid Bi are given in Table 2. The average value of  $\Gamma$  from Table 2 is  $(9.2 \pm 0.6) \times 10^{-8} \text{ Km}$  for solid Bi in equilibrium with the Bi–Ag eutectic liquid.

### Determination of entropy of fusion per unit volume

In order to determine the solid–liquid interfacial energy, it is also necessary to know the entropy change per unit volume,  $\Delta S^*$  for solid phase.

The effective entropy change per unit volume,  $\Delta S^*$ , for a two-component system is

$$\Delta S^* = \frac{RT(X_{S\infty} - C_{L\infty})}{m_L(1 - C_{L\infty})C_{L\infty}V_S} \quad (5)$$

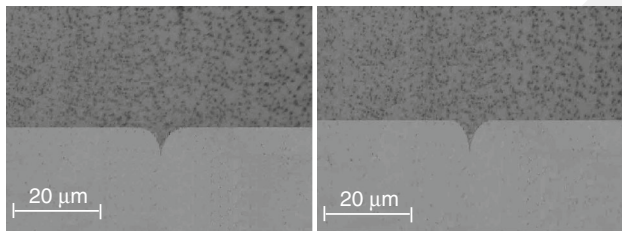
The molar volume,  $V_s$ , is expressed as

$$V_s = V_c N \frac{1}{n} \quad (6)$$

where  $V_c$  is the volume of the unit cell,  $N$  is the Avogadro’s number and  $n$  is the number of atoms per unit cell. The crystal structure of solid Bi solution is trigonal with  $a = 4.55 \times 10^{-10} \text{ m}$  and  $c = 11.85 \times 10^{-10} \text{ m}$ . The volume of trigonal is determined with

**Table 1** Thermal conductivities of solid and liquid phases for Bi-based binary or ternary alloys at their melting temperature

Alloy	Phases	Melting temperature/K	K/W K <sup>-1</sup> m <sup>-1</sup>	$R = K_l K_s^{-1}$	
Bi–Ag (PW)	Eutectic liquid (Bi–4.7 at.%Ag)	534.75	9.19	0.88	
	Eutectic Solid (Bi–4.7 at.%Ag)		10.44		
	Eutectic liquid (Bi–4.7 at.%Ag)		9.19	1.45	
	Solid Bi		6.35 [13]		
Bi–Al–Zn [21]	Liquid (Bi–8.04 at.%Zn–0.38 at.%Al)	527.15	13.85	1.34	
	Solid (Bi–6.1 at.%Zn–0.38 at.%Al)		10.34		
Bi–In [19]	Eutectic Liquid (Bi–52.7 at.%In)	382.65	10.60	0.80	
	Eutectic solid (Bi–52.7 at.%In)		13.25		
	Eutectic liquid (Bi–52.7 at.%In)		10.60	1.27	
	Solid Bi		8.35		
Bi–Cd [20]	Liquid Bi–55.04 at.%Cd	418.70	10.06	0.81	
	Solid Bi–55.04 at.%Cd		12.46		
	Liquid Bi–55.04 at.%Cd		10.06		1.24
	Solid Bi		8.12		

**Fig. 3** Typical grain boundary groove shapes for solid Bi in equilibrium with Bi–4.7 at.%Ag eutectic liquid

$$V_c = (\sqrt{3}/2)a^2c \quad (7)$$

Thus the molar volume of solid Bi solution is found to be  $21.31 \times 10^{-6} \text{ m}^3$ . The values of the relevant constant used in the determination of entropy of fusion per unit volume were obtained from phase diagram [12] and are given in Table 3. The error in the determination of entropy of fusion per unit volume is estimated to be about 5 % [22].

### Evaluation of the solid–liquid interfacial energy

If the values of  $\Gamma$  and  $\Delta S^*$  are known, the value of solid–liquid interfacial energy,  $\sigma_{sl}$ , can be evaluated from Eq. 3. The solid–liquid interfacial energy of the solid Bi in equilibrium with the eutectic liquid was evaluated to be

**Table 2** Gibbs–Thomson coefficients for solid Bi in equilibrium with Bi–Ag eutectic liquid

Grove no.	$G_k \times 10^2/\text{Km}^{-1}$	$\alpha^\circ$	$\beta^\circ$	Gibbs–Thomson coefficient	
				$\Gamma_{\text{lhs}} \times 10^{-8}/\text{Km}$	$\Gamma_{\text{rhs}} \times 10^{-8}/\text{Km}$
a	107.0	13.3	12.3	9.6	9.4
b	106.1	16.7	12.6	9.0	9.4
c	107.5	13.8	13.8	9.4	9.5
d	106.7	11.2	12.0	9.0	9.4
e	104.7	11.8	14.3	9.1	9.0
f	104.6	10.3	11.2	9.3	9.3
g	105.5	11.2	11.2	9.2	9.3
h	108.2	12.8	11.8	9.2	9.0
i	106.7	12.3	12.3	9.3	9.1
j	106.1	12.6	14.1	9.4	9.4

$\bar{\Gamma} = (9.2 \pm 0.6) \times 10^{-8} \text{ Km}$

Subscripts lhs and rhs refer to left-hand side and right-hand side of groove, respectively

$(52.7 \pm 6.3) \times 10^{-3} \text{ J m}^{-2}$  using the values of  $\Gamma$  and  $\Delta S^*$ . The experimental error in the determination of solid–liquid interfacial energy is the sum of experimental errors of the Gibbs–Thomson coefficient and the entropy change of fusion per unit volume. Thus, the total experimental error in the evaluation of solid–liquid interfacial energy evaluation in present work is estimated to be about 12 %.

### Determination of grain boundary energy

By considering a force balance at the grain boundary groove, it is possible to determine the solid–solid interface energy and grain boundary energy provided that the solid–liquid interface energy is known. From the force balance at the grain boundary groove shape in [8], the grain boundary energy can be expressed as

$$\sigma_{\text{gb}} = 2\sigma_{\text{sl}} \cos \theta \quad (8)$$

where

$$\theta = \frac{\theta_a + \theta_b}{2} \quad (9)$$

is the angle that the solid–liquid interfaces make with the  $y$  axis.

The value of the grain boundary energy for the solid Bi was found to be  $(102.4 \pm 13.3) \times 10^{-3} \text{ J m}^{-2}$  using the values of the  $\sigma_{\text{sl}}$  and  $\theta$  in Eq. 8. The estimated error in determination of  $\theta$  angles was found to be 1 %. Thus the total experimental error in the resulting grain boundary energy is about 13 %.

A comparison of the values of Gibbs–Thomson coefficient ( $\Gamma$ ), solid–liquid interface energy ( $\sigma_{\text{sl}}$ ) and grain boundary energy ( $\sigma_{\text{gb}}$ ) for solid Bi in the Bi–Ag eutectic system obtained in present work with the values of  $\Gamma$ ,  $\sigma_{\text{sl}}$  and  $\sigma_{\text{gb}}$  for solid Bi in the different binary or ternary alloy

**Table 3** Some physical properties of solid Bi phase in the Bi–Ag alloy

System Bi–Ag	
Concentration of solid phase $C_s$	Solid Bi [12] (Bi–2.87 at.%Ag)
Concentration of liquid phase $C_l$	Eutectic liquid [12] (Bi–4.7 at.%Ag)
$f(C)^a$	1.04 [12]
Melting temperature, $T_m/\text{K}$	534.75 [12]
Molar volume of solid Bi, $V_{\text{Bi}} \times 10^{-6}/\text{m}^3$	21.31 [19]
Liquidus slope of solid Bi, $m_l/\text{Kat.fr}^{-1}$	382.36 [12]
Entropy change in fusion for solid Bi, $\Delta S^*/\text{J K}^{-1} \text{m}^{-3}$	$5.7 \times 10^5$

<sup>a</sup>  $f(C) = \frac{C_s - C_l}{(1 - C_l)C_l}$

**Table 4** Comparison of the values of  $\Gamma$ ,  $\sigma_{\text{sl}}$ ,  $\sigma_{\text{gb}}$  for solid Bi phase measured in present work with the values of  $\Gamma$ ,  $\sigma_{\text{sl}}$ ,  $\sigma_{\text{gb}}$  for solid Bi phases in the Bi-based binary and ternary systems obtained in previous works

System	Solid phase	Liquid phase	Temp./K	Molar volume of solid $V_s \times 10^{-6}/\text{m}^3$	Entropy change in fusion $\Delta S^* \times 10^5/\text{J K}^{-1} \text{m}^{-3}$	Gibbs–Thomson coefficients $\Gamma \times 10^{-8}/\text{Km}$	Solid–liquid interface energy $\sigma_{\text{sl}} \times 10^{-3}/\text{J m}^{-2}$		Grain boundary energy $\sigma_{\text{gb}} \times 10^{-3}/\text{J m}^{-2}$
							Theoretical	Experimental	
Bi	Bi	Bi	544.40	–	–	–	59.2 [27]	79.3 CNE [26]	–
							68 [29]	60.2 CNE [23]	
								74 $\pm$ 3 DAM [25]	
								55–80 DMP [24]	
Bi–Cd	Bi	Bi–54.6at.%Cd [28]	418.70	42.71 [30]	6.99 [30]	10.3 $\pm$ 0.4 [20]		72.1 $\pm$ 10.1 [20]	140.5 $\pm$ 21.1 [20]
Bi–In	Bi	Bi–47.3at.%In [28]	382.65	21.31 [31]	6.43 [19]	8.4 $\pm$ 0.4 [19]		54.0 $\pm$ 5.4 [19]	105.5 $\pm$ 11.6 [19]
Bi–Al–Zn	Bi	Bi–8.04 at.%Zn–0.38 at.%Al	527.15	21.31 [31]	6.0 [21]	9.1 $\pm$ 0.6 [21]		54.9 $\pm$ 6.6 [21]	100.0 $\pm$ 13.0 [21]
Bi–Ag [PW]	Bi	Bi–4.7 at.%Ag	534.75	21.31 [31]	5.7	9.2 $\pm$ 0.6		52.7 $\pm$ 6.3	102.4 $\pm$ 13.3

PW present work, CNE classical nucleation experiments, DAM dihedral angle measurement, DMP depression of melting point, GBG grain boundary groove method

systems determined in previous works [19–21, 23–31] is given in Table 4.

As mentioned above, interfacial energy anisotropy is considered to play a critical role in many phase transformations. The accurate determination of these quantities remains a challenge, and reported investigations are limited. The anisotropy of solid–liquid interfacial energy for bismuth is about 26 % [22]. The estimated experimental error in measurement of solid–liquid interfacial energy in the present work is about 13 %. In present work, the solid–liquid interfacial energy was assumed to be isotropic and the average value of solid–liquid interfacial energy was obtained. As can be seen from Table 4, the results obtained in present work for solid Bi in the Bi–Ag eutectic alloy agree with the results obtained in previous works for solid Bi in the different binary or ternary alloys [19–21, 23–31] in the limits of experiment errors.

## Conclusions

A radial temperature gradient on the sample was established by heating from the centre with a single heating wire and cooling the outside of the sample with a heating/refrigerating circulating bath. The equilibrated grain boundary groove shapes for solid Bi in the Bi–Ag eutectic alloy were observed from a quenched sample. To evaluate the thermodynamic properties such as the Gibbs–Thomson coefficient, solid–liquid interfacial energy and grain boundary energy of solid Bi in the Bi–Ag eutectic system from the observed grain boundary groove shapes, the thermal conductivity of solid Bi and thermal conductivity of Bi–Ag eutectic liquid at their melting temperature were measured with radial heat flow and Bridgman-type directional solidification methods, respectively. The Gibbs–Thomson coefficient, solid–liquid interfacial energy and grain boundary energy of solid Bi in equilibrium with Bi–Ag eutectic liquid were then determined from observed grain boundary groove shapes by using the measured values of thermodynamic properties for Bi–Ag eutectic system. The results obtained in present work for Bi–Ag eutectic alloy were compared with the results obtained in previous works for solid Bi in the different binary or ternary alloys [19–21, 23–31]. It was seen that the results obtained in present work for solid Bi in the Bi–Ag eutectic alloy agree with the results obtained in previous works [19–21, 23–31] for solid Bi in the different binary or ternary alloys in the limits of experiment errors.

**Acknowledgements** This project was supported by Erciyes University Scientific Research Project Unit under Contract No: FBA–2013–4746. The authors are grateful to Erciyes University Scientific Research Project Unit for their financial supports. Yemliha Altıntas would like to thank to TUBITAK for support through a scholarship.

## References

- Eustathopoulos N, Nicholas MG, Drevet B. Wettability at high temperatures. Oxford: Pergamon Materials Series; 1999.
- Martin JW, Doherty RD, Cantor B. Stability of microstructure in metallic systems. Cambridge: Cambridge University Press; 1997.
- Jones DRH, Chadwick GA. Experimental measurement of solid–liquid interfacial energies: the ice water–sodium chloride system. *J Cryst Growth*. 1971;11:260–4.
- Schaefer RJ, Glicksman ME, Ayers JD. High confidence measurement of solid/liquid surface energy in a pure material. *Phil Mag*. 1975;32:725–43.
- Hardy SC. A grain boundary groove measurement of the surface tension between ice and water. *Phil Mag*. 1977;35:471–84.
- Gündüz M, Hunt JD. The measurement of solid–liquid surface energies in the Al–Cu, Al–Si and Pb–Sn systems. *Acta Metall*. 1985;33:1651–72.
- Maraşlı N, Hunt JD. Solid–liquid surface energies in the Al–CuAl<sub>2</sub>, Al–NiAl<sub>3</sub> and Al–Ti systems. *Acta Mater*. 1996;44:1085–96.
- Keşlioğlu K, Gündüz M, Kaya H, Çadırlı E. solid–liquid interfacial energy in the Al–Ti system. *Mater Lett*. 2004;58(24):3057–73.
- Akbulut S, Ocak Y, Keşlioğlu K, Maraşlı N. Thermal conductivities of solid and liquid phases for neopentylglycol, aminomethylpropanediol and their binary alloy. *J Phys Chem Solids*. 2009;70(1):72–8.
- Ocak Y, Akbulut S, Keşlioğlu K, Maraşlı N. solid–liquid interfacial energy of neopentylglycol. *J Colloid Interface Sci*. 2008;320(2):555–62.
- Trivedi R, Hunt JD. The mechanics of solder alloy wetting and spreading. New York: Van Nostrand, Reinhold; 1993. p. 191.
- Li Z, Cao Z, Knott S, Mikula A, Du Y, Qiao Z. Thermodynamic investigation of the Ag–Bi–Sn ternary system. *CALPHAD*. 2008;32:152–63.
- Touloukian YS, Powell RW, Ho CY, Klemensi PG. Thermal conductivity metallic elements and alloys. vol. 1, Plenum, New York; 1970. pp. 10–14.
- Porter DA, Easterling KE. Phase transformations in metals and alloys. Van Nostrand Reinhold Co. Ltd, UK; 1991. pp. 204.
- Mccartney DG. D.Phil. thesis, University of Oxford, UK; 1981. pp. 85
- Ersoy SB, Altıntas Y, Karadağ SB, Aksöz S, Keşlioğlu K, Maraşlı N. Solid–liquid interfacial energy of solid succinonitrile in equilibrium with succinonitrile–1,4–diiodobenzene eutectic liquid. *J Therm Anal Calorim*. 2015;119:1867–74.
- Bayram Ü, Aksöz S, Maraşlı N. Temperature dependency of thermal conductivity of solid phases for fatty acids. *J Therm Anal Calorim*. 2014;118:311–21.
- Altıntas Y, Öztürk E, Aksöz S, Keşlioğlu K, Maraşlı N. The experimental determination of interfacial energies for solid Sn in equilibrium with Sn–Mg–Zn liquid. *Met Mater Int*. 2015;21–2:286–94.
- Ocak Y, Akbulut S, Maraşlı N, Keşlioğlu K, Büyük U, Kaya H, Çadırlı E. Interfacial energy of solid bismuth in equilibrium with Bi–In eutectic liquid at 109.5 °C equilibrating temperature. *Met Mater Int*. 2008;14:177–87.
- Erol M, Maraşlı N, Keşlioğlu K, Gündüz M. Solid–liquid interfacial energy of bismuth in the Bi–Cd eutectic system. *Scr Mater*. 2004;51:131–5.
- Aksöz S, Ocak Y, Keşlioğlu K, Maraşlı N. Thermal conductivity and interfacial energy of solid Bi solution in the Bi–Al–Zn eutectic system. *Fluid Phase Equilib*. 2010;293:32–41.
- Tassa M, Hunt JD. The measurement of Al–Cu dendrite tip and eutectic interface temperatures and their use for predicting the extent of the eutectic range. *J Cryst Growth*. 1976;34:38–48.

23. Skripov VP. Homogeneous nucleation in metals and amorphous films. In: Kaldis E, Schell H, editors. *Crystal growth and materials*, vol. 327. Amsterdam: North Holland; 1977.
24. Glicksman ME, Vold CI. Determination of absolute solid–liquid interfacial free energies in metals. *Acta Met.* 1969;17:1–11.
25. Glicksman ME, Vold CI. Establishment of error limits on the solid–liquid interfacial free energy of bismuth. *Scr Met.* 1971; 5:493–8.
26. Prepežko JH, Rasmussen KH, Anderson IE, Loper CR. *Undercooling of low-melting metals and alloy solidification and casting of metals*, vol. 169. London: Metals Society; 1979.
27. Waseda Y, Miller WA. Calculation of the crystal–melt interfacial free energy from experimental radial distribution function data. *Trans Japan Inst Met.* 1978;19:546–52.
28. Hansen M, Anderko K. *Constitutions of binary alloys*. New York: McGraw-Hill Book Company; 1958. p. 303.
29. Kotze IA, Kuhlmann-Wilsdorf DJ. A theory of the interfacial energy between a crystal and the melt. *Appl Phys Lett.* 1966;9:96–8.
30. Suryanarayana C, Norton MG. *X-ray diffraction—a practical approach*. New York: Plenum Press; 1998. p. 252.
31. Hengli L, Lizhu S, Muyu Z. Excess molar volumes of lead-based  $\alpha$ -phase solid solutions in (lead + bismuth + indium) at 298.15 K. *J Chem Therm.* 1990;22:821–6.

GCRIIS